A way to limit the corrosion in the Molten Salt Reactor concept: the salt redox potential control

M. Gibilaro *, L. Massot, P. Chamelot

Université de Toulouse, UPS, CNRS, Laboratoire de Génie Chimique, 118 Route de Narbonne, F-31062 Toulouse, France

A B S T R A C T

The possibility of controlling the salt redox potential thanks to a redox buffer in the Molten Salt Fast Reactor was investigated, the goal was to limit the oxidation of the reactor structural material. Tests were performed in LiF-CaF_2 at 850 °C on two different redox couples to fix the salt potential, Eu(III)/Eu(II) and U(IV)/U(III), where the first one was used as inactive system to validate the methodology to be applied on the uranium system. A metallic reducing agent (Gd plate for Eu, and U plate for U system) was inserted in the salt, leading to a spontaneous reaction: Eu(III) and U(IV) were then reduced. Eu(III) was fully converted into Eu(II) with metallic Gd, validating the approach. On the U system, the U(IV)/U(III) ratio has to be set between 10 and 100 to limit the core material oxidation: addition of metallic U decreased the concentration ratio from the infinite to 1, showing the feasibility of the salt redox potential control with the U system.

1. Introduction

Generation IV International Forum (GIF) identified and selected six nuclear energy systems based on four broad areas: sustainability, economics, safety and reliability, proliferation resistance and physical protection [1]. Among them, the Molten Salt Fast Reactor (MSR) represents one of the most promising option as it can be used as transmuter, to burn plutonium and other transuranic elements. The MSFR originality is the use of a liquid fuel made of a molten fluoride circulating in both reactor core and heat exchanger: the fission material, ^{233}U, is dissolved in this carrier salt, and used as a heat-transferring agent.

The MSR development started in the Oak Ridge National Laboratory (ORNL) in the US with the military Aircraft Nuclear Propulsion Program in the 1950s [2]. This novel technology was then turned to civilian applications with the construction of the Molten Salt Reactor Experiment (MSRE) in the 1960s, operated with LiF-BeF_2-ZrF_4-UF_4 and the Molten Salt Breeder Reactor (MSBR) in the 1970s, with LiF-BeF_2-ThF_4-UF_4 [3,4]. ORNL demonstrated few decades ago the feasibility of the molten salt nuclear reactor concept. During reactor operation time, plethora of information were recorded and experiments evidenced the excellent compatibility and the good corrosion resistance of Hastelloy-N with molten fluoride system at 650 °C [5]. Moreover, post-operative examination of the reactor container material showed that corrosion was successfully minimised by the control of the redox potential of the salt [6].

To regulate the redox conditions of the salt, a buffer couple was used: U(IV)/U(III). The redox potential of the salt is thus fixed by the uranium redox couple thanks to the Nernst law:

$$E_{salt} = E^{\circ}_{U(IV)/U(III)} + \frac{RT}{F}\ln\left(\frac{[U(IV)]}{[U(III)]}\right) \quad (1)$$

Where E° is the standard potential of U(IV)/U(III) couple (V), R the ideal gas constant (J/K/mol), F the Faraday constant (C/mol) and [x] the concentration of the x species (mol/L).

Two different redox conditions are expected [7]:

- either the salt redox potential is too reducing; in this case, two options have to be examined:

○ carbon is present in the core and may react with uranium to form carbides as described below:

$$4U(III) + xC = 3U(IV) + UC_x \quad (2)$$

○ carbon is absent from the core: the tritium, produced by fission as TF, is reduced into gaseous tritium (T_2) and might diffuse through the structural material [8].

- or the salt redox potential is too oxidizing: the core material is corroded and the dissolution of a metal M is observed.

In the MSFR concept, a carbon-free structure was selected. For the core material, hastelloy-N is a good candidate and is a Ni-base alloy (68%) which contains around 17% Mo, 7% Cr, 5% Fe and 1% Mn. As the most reactive element is Cr, the structural material oxidation in a uranium fuelled system would be [9]:

$$Cr + 2U(IV) = 2U(III) + Cr(II) \quad (3)$$

To avoid it, a careful selection of U(IV) and U(III) concentrations has to be done and has been described in [10]. To define the lower and upper range of this ratio, different assumptions were taken into account:

- the lower limit was set to 10, corresponding to the solubility limit of U(III)
- the upper limit was correlated to an acceptable chromium corrosion rate.

According to calculation from Fig. 1 representing the mole fraction of dissolved Cr(II) as a function of temperature, the redox potential control won't prevent the oxidation of chromium: whatever the uranium ratio, Cr dissolution takes place. However, it is still possible to limit it: with a ratio set to 100, the mole fraction of dissolved Cr(II) in the salt becomes reasonable. To resume, the uranium concentration ratio should be set between 10 and 100.

However, during the reactor operation time, it was shown that the average of the total valence of the fission products is slightly less than four, resulting in the gradual conversion of U(III) to U (IV). This leads to an increase of the [U(IV)]/[U(III)] ratio and of the reactor vessel corrosion: the salt tends to be more and more acid and a periodic adjustment of redox conditions is thus necessary [11].

To decrease the redox potential, a reducing metal is added in the salt to spontaneously consume U(IV). The choice of the reducing agents (R) in MSRE and MSBR was limited to metals whose cations were initially present in the molten fluoride mixture, e.g. Be or Zr:

$$xU(IV) + R = xU(III) + R(X) \quad (4)$$

To get rid of some drawbacks (use of graphite and Be for instance), the Molten Salt Fast Reactor was developed by the CNRS in France [12]. The fuel is then a mixture of LiF, ThF_4 and UF_4 and the reducing metal could be either Th or U.

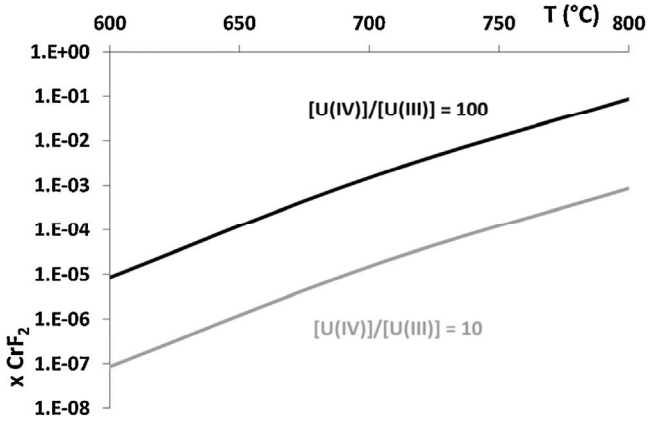

Fig. 1. Mole fraction of dissolved CrF_2 as a function of temperature for two different uranium concentration ratios.

In this work, tests on redox potential control were performed in the eutectic LiF-CaF_2 at 850 °C. A first system was studied: Eu (III)/Eu(II) couple with metallic Gd as reducing agent. A Gd plate was inserted to spontaneously convert Eu(III) into Eu(II) as follows:

$$3Eu(III) + Gd = 3Eu(II) + Gd(III) \quad (5)$$

Electrochemical methods were used to record the redox potential change, imposed by [Eu(III)]/[Eu(II)], by cyclic voltammetry on silver and molybdenum electrodes. The Eu(III) concentration decrease and, the Eu(II) and Gd(III) concentrations increase were observed.

After validation of the method, tests on active material were performed on the U(IV)/U(III) redox couple. Metallic uranium was chosen as reducing agent, leading to the following spontaneous reaction:

$$3U(IV) + U = 4U(III) \quad (6)$$

Cyclic voltammetries were realised on a silver electrode for different U plate immersion time, to detect the changes of uranium ions concentration. Finally, the U(IV)/U(III) concentration ratio was estimated and the salt redox potential controlled.

2. Experimental part

2.1. Techniques

All electrochemical studies were performed with an Autolab PGSTAT 30 potentiostat/galvanostat controlled by a computer using the research software GPES 4.9.

A classical three electrodes set up was used to perform electrochemical measurements; the reference electrode was a Pt wire (quasi reference electrode $Pt/PtO_x/O^{2-}$), the counter electrode was a glassy carbon rod and two kinds of working electrodes were used: Mo and Ag wires ($\varphi = 1$ mm).

Contents of elements (Eu, Gd, U) were measured, after dissolution in an equimolar mixture of pure nitric and hydrochloric acids, using Inductively Coupled Plasma–Atomic Emission Spectroscopy (ICP-AES, HORIBA Ultima 2).

2.2. The cell

The cell was a vitreous carbon crucible placed in a cylindrical vessel made of refractory steel and closed by a stainless steel lid cooled by circulating water. The inside part of the walls was protected against fluoride vapours by a graphite liner. The experiments were performed under an inert argon atmosphere (less than one ppm O_2). The cell was heated using a programmable furnace and the temperatures were measured using a chromel-alumel thermocouple.

2.3. Solutes/Salts

Solutes were introduced as powder in the cell, UF_4 and EuF_3 (purity > 99.9%), and stored in glovebox under argon atmosphere, as the U and Gd metallic plates (2 cm × 8mm × 2 mm): the surface area is then $S = 1.6\ cm^2$.

The electrolytic bath consisted of a eutectic LiF-CaF_2 (Carlo Erba Reagents 99.99%) mixture (79.5/20.5 molar ratio), initially dehydrated by heating under vacuum (10^{-5} bar) to its melting point for 72 hours and the electrolyte volume is $V = 100\ cm^3$.

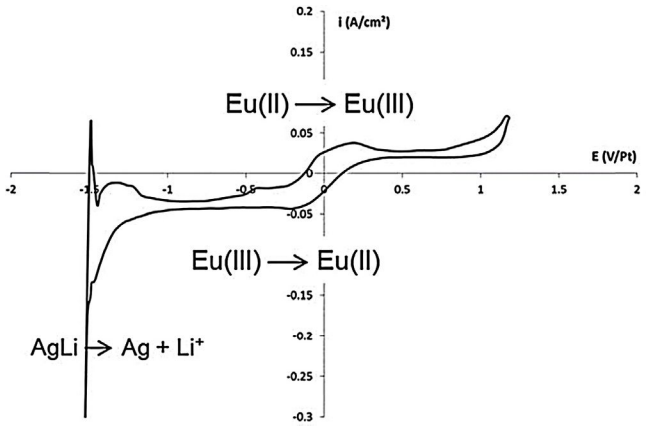

Fig. 2. Cyclic voltammetry on Ag in LiF-CaF_2 + EuF_3 (2.5 wt%) at 850 °C at 50 mV.s^{-1}; Scan direction: from the initial potential (E = 0 V/Pt) to the electrode oxidation.

3. Results and discussion

3.1. Inactive system: Eu(III)/Eu(II)

Before starting with active material, a preliminary test was done on the europium redox couple. The goal was to test the system response and to validate the experimental approach.

Addition of 2.5 wt% of europium fluoride (III) was made in LiF-CaF_2 and the Eu concentration checked by ICP-AES. A typical cyclic voltammetry is presented in Fig. 2 on a silver electrode at 850 °C. Addition of EuF_3 in the salt leads to an equilibrium between the Eu (III) and the Eu(II) species [13], very similar to the targeted system U(IV)/U(III): two species (defining the redox couple) are present in the solution and impose the redox potential of the salt (Nernst law).

Two electrochemical reactions for Eu species are expected:

- Reduction reaction (I < 0): $Eu(III) + 1e^- \rightarrow Eu(II)$ (7)
- Oxidation reaction (I > 0): $Eu(II) \rightarrow Eu(III) + 1e^-$ (8)

It can be noticed that the metallic Eu deposition is impossible in LiF-CaF_2 [13] and that, in the case of a silver electrode in LiF-CaF_2, the solvent reduction is not metallic Li but an Ag-Li alloy.

A Gd plate was then inserted into the melt and a spontaneous reaction between Eu(III) and Gd took place:

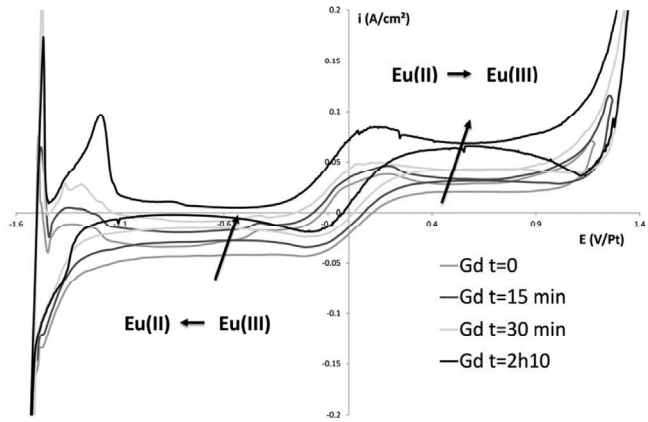

Fig. 3. Cyclic voltammetry on Ag in LiF-CaF_2 + EuF_3 (2.5 wt%) + Gd at 850 °C at 50 mV.s^{-1}; Scan direction: from the initial potential (E = 0 V/Pt) to the electrode oxidation.

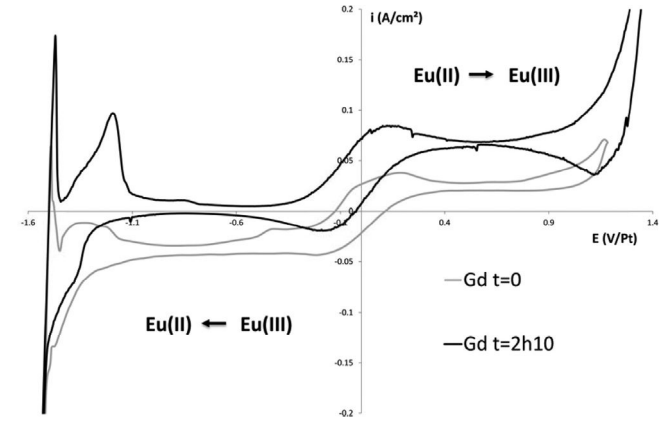

Fig. 4. Cyclic voltammetry on Ag in LiF-CaF_2 + EuF_3 (2.5 wt%) + Gd at 850 °C at 50 mV.s^{-1}; Scan direction: from the initial potential (E = 0 V/Pt) to the electrode oxidation.

$$3Eu(III) + Gd = 3Eu(II) + Gd(III) \quad (5)$$

The methodology was the following: the Gd plate was dipped in the salt for a defined time period and a cyclic voltammetry was periodically recorded. Fig. 3 shows the evolution of the cyclic voltammograms during the conversion process of Eu(III) into Eu(II) in our experimental conditions (electrode surface area S/solution volume V: S/V = 16.10^{-3} $cm^2.cm^{-3}$).

In agreement with Eq. (5), a decrease of the Eu(III) reduction current density and an increase of the Eu(II) oxidation current density are observed, corresponding to a decrease of [Eu(III)] and an increase of [Eu(II)]. An overlay of the initial and the final signal is plotted in Fig. 4.

After 2h10, no more Eu(III) is present in the salt and a total conversion of Eu(III) into Eu(II) is observed: the reduction current density of Eu(III) is equal to zero.

Moreover, a mass balance on Eu species shows that the reaction is total, in agreement with Eq. (5):

$$I^{final}_{Eu(III)/Eu(II)} = I^{t=0ox}_{Eu(III)/Eu(II)} + I^{t=0red}_{Eu(III)/Eu(II)} \quad (9)$$

On an inert Mo electrode (Fig. 5), a new electrochemical signal appears during the conversion process at −2 V/Pt and is attributed to the Gd(III)/Gd system [14], as expected from Eq. (5): more the Gd plate is in the bath, more the intensity of the Gd(III) reduction increases. Gd concentration in the bath was titrated by ICP-AES and

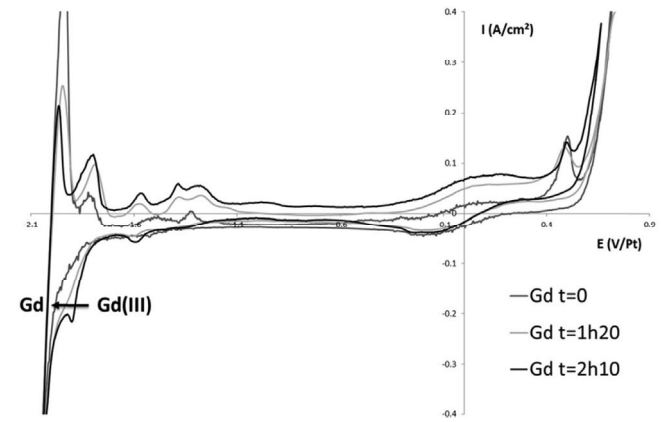

Fig. 5. Cyclic voltammetry on Mo in LiF-CaF_2 + EuF_3 (2.5 wt%) + Gd at 850 °C at 50 mV.s^{-1}; Scan direction: from the initial potential (E = −0.1 V/Pt) to the electrode oxidation.

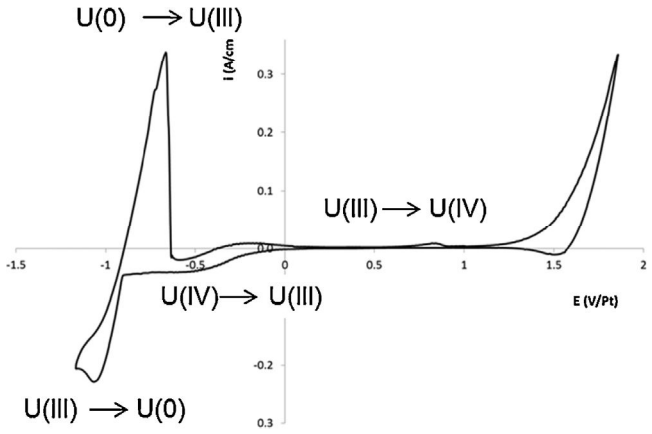

Fig. 6. Cyclic voltammetry on Ag in LiF-CaF_2 + UF_4 (3.5 wt%) at 850 °C at 50 mV.s^{-1}; Scan direction: from the initial potential (E = −0.25 V/Pt) to the electrode oxidation.

is in agreement with the spontaneous reaction between Gd and Eu (III) (Eq. (5)).

These preliminary tests validate the methodology and U(IV)/U (III) redox couple was investigated.

3.2. Active system: U(IV)/U(III)

The methodology developed for Eu was applied to the uranium system. In Fig. 6 is presented a typical cyclic voltammogram obtained after UF_4 addition (3.5 wt.%, titrated by ICP-AES) on silver electrode at 850 °C in LiF-CaF_2.

The signal highlights different electrochemical reactions:

- Reduction reactions: $U(IV) + 1e^- \rightarrow U(III)$ (10)

$$U(III) + 3e^- \rightarrow U \quad (11)$$

- Oxidation reactions: $U(III) \rightarrow U(IV) + 1e^-$ (12)

$$U \rightarrow U(III) + 3e^- \quad (13)$$

The initial solution was only composed of U(IV), and to transform it into U(III), an U plate was inserted into the molten

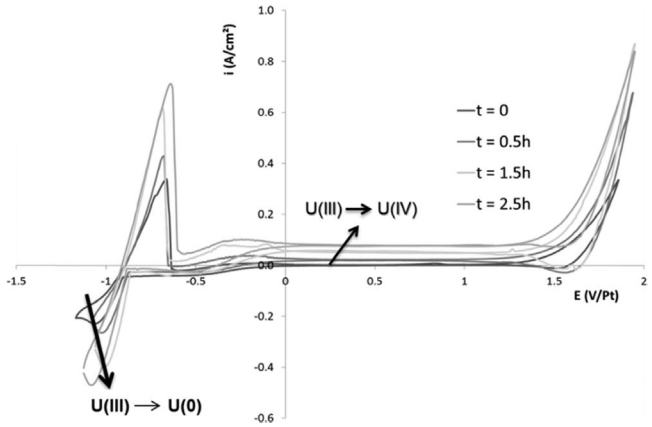

Fig. 7. Cyclic voltammetries on Ag in LiF-CaF_2 + UF_4 (3.5 wt%) + U at 850 °C at 50 mV. s^{-1}; Scan direction: from the initial potential (E = −0.25 V/Pt) to the electrode oxidation.

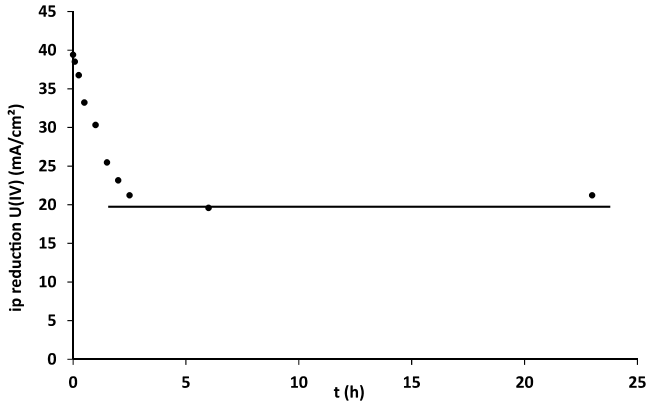

Fig. 8. Reduction current density of U(IV) plotted versus the U immersion time at 850 °C.

solvent (S/V = 16.10^{-3} $cm^2.cm^{-3}$). A spontaneous reaction between U and U(IV) was observed:

$$3U(IV) + U = 4U(III) \quad (6)$$

Cyclic voltammograms were recorded at different time of U immersion and overlaid in Fig. 7. As expected from Eq. (6), the U plate immersion into the molten solution leads to:

- a decrease of the U(IV) reduction current density
- an increase of the U(III) reduction current density
- and an increase of the U(III) oxidation current density

The U(IV) conversion into U(III) is thus effective: the U(IV) concentration decreases and the U(III) concentration increases. Surprisingly, no more change in the electrochemical recording was detected after 2.5 h: moreover, the signal remained stable for days. An equilibrium was thus reached as no more U(IV) was reduced. To investigate this situation, the reduction current density of U(IV) was plotted versus the U immersion time in Fig. 8: it showed that the U(IV) reduction current density reaches a limiting value of 20 mA/cm^2 in 2.5 h.

The U(IV) reduction being controlled by the symproportionation reaction in Eq. (6), the related thermodynamic equilibrium constant is defined as:

$$K = \frac{a^4_{U(III)}}{a^3_{(IV)}} \quad (14)$$

Where a_x is the activity of the species x.

After 2.5 h, the reaction stops, meaning that the equilibrium is reached: activities of each species correspond to the ratio defined by K (Eq. (14)). Unfortunately, the activity coefficients are missing to estimate this value.

To calculate the [U(IV)]/[U(III)] ratio obtained at the equilibrium, U(IV) and U(III) concentrations have to be known.

Table 1
Estimation of the U(IV)/U(III) concentration ratios at 850 °C.

time (hour)	[U(IV)] mol/L	[U(III)] mol/L	U(IV)/U(III) ratio
0	2.25E-01	0	/
0.08	2.20E-01	9.00E-03	24.44
0.25	2.10E-01	2.20E-02	9.55
0.5	1.90E-01	4.72E-02	4.02
1	1.73E-01	6.93E-02	2.50
1.5	1.46E-01	1.06E-01	1.37
2	1.32E-01	1.24E-01	1.07
2.5	1.21E-01	1.39E-01	0.87

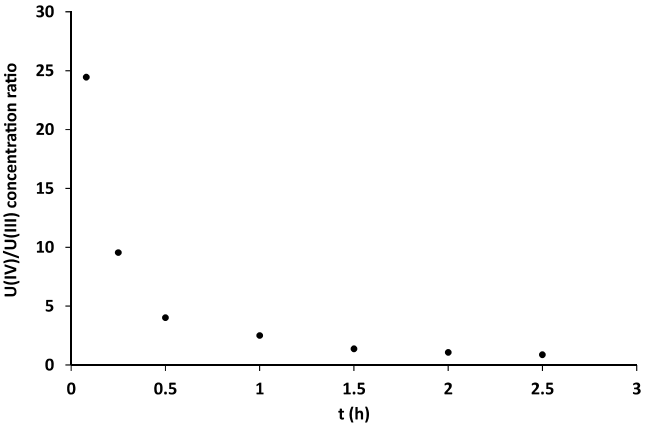

Fig. 9. U(IV)/U(II) concentration ratio versus the U immersion time at 850 °C.

The U(IV) concentration can be evaluated thanks to a calibration curve, relating the peak current density and the U(IV) concentration in LiF-CaF_2 at 850 °C [15].

Then, the U(III) concentration was estimated with a mass balance on uranium, according to Eq. (6):

$$[U(III)]_t = \frac{4}{3}\{[U(IV)]_{t=0} - [U(IV)]_t\} \quad (15)$$

Where $[x]_{t=0}$ is the initial concentration of x (mol/L) and $[x]_t$ the concentration of x at the time t (mol/L)

The concentration values of both uranium species are gathered in Table 1, as well as the uranium concentration ratios. Although the S/V ratio is very low (16.10^{-3} $cm^2.cm^{-3}$), the conversion kinetics of U(IV) into U(III) is very fast: the ratio goes from the infinite at the beginning, to 4 within half an hour as presented in Fig. 9. The most important conclusion is that an equilibrium is obtained in 2.5 h in our experimental conditions and corresponds to a uranium concentration ratio of 1. As it should be set between 10 and 100 to avoid the core material corrosion, the redox potential of the salt is thus achievable using a U plate as reducing agent.

4. Conclusions

The main goal was to look at the opportunity to control the salt redox potential thanks to a redox buffer, to limit the corrosion of the structural material. Tests were performed in LiF-CaF_2 at 850 °C on two different systems with both two species in equilibrium in solution which fixed the salt redox potential: Eu(III)/Eu(II) and U(IV)/U(III). The first couple was used to validate the methodology on inactive material and then to apply it on the uranium system.

To control the core material consumption, the recommended U(IV)/U(III) concentrations ratio should be in between 10 and 100. A reducing agent was dipped into the salt (Gd or U) and the concentration change of the solutes was detected by electrochemical measurements. The two spontaneous reactions occured:

$$3Eu(III) + Gd = 3Eu(II) + Gd(III)$$

$$3U(IV) + U = 4U(III)$$

On the europium system, Eu(III) was fully converted into Eu(II) using a Gd plate, validating the approach. Then the U(IV)/U(III) couple was investigated using a metallic U plate. The kinetics of U(IV) reduction was very fast and an equilibrium between U(IV)/U(III) and U(III)/U was quickly reached (2.5 h for S/V = 16.10^{-3} $cm^2.cm^{-3}$). The U(IV)/U(III) concentration ratios were evaluated, knowing the initial concentration of U(IV) and using a mass balance for U(III) concentration determination. Results showed that the initial ratio tended towards infinity (only U(IV) was present) and that it was possible to decrease it to 1.

As the goal was to set the ratio between 10 and 100, the redox potential control of the salt is thus feasible with a uranium plate. Two options are then possible:

- A control of the U plate immersion time; however, as the conversion kinetics is very fast, the operation will be hard to control.
- Or addition of a defined quantity of metallic U to convert the desired amount of U(IV), which is easier to realise and seems to be the best option. Then, corrosion tests have to be performed on selected materials for different salt redox potentials to demonstrate the structural material resistance.

Acknowledgment

This work was supported by the European EVOL (FP7-CT-2010-249 696) program.

References

[1] A Technology Roadmap for Generation IV Nuclear Energy Systems, US DOE Nuclear Research Advisory Committee and Generation IV International Forum, 2002, available on https://www.gen-4.org/gif/jcms/c_42188/publications.
[2] W.H. Jordan, S.J. Cromer, A.J. Miller, ORNL 2387 (1958) .
[3] W.R. Grimms, Nucl. Appl. & Techn 8 (1970) 137–155.
[4] P.N. Haubenreich, J.R. Engel, Nucl. Appl. & Techn. 8 (1970) 118–136.
[5] H.E. McCoy, Nucl. Appl. & Techn. 8 (1970) 156–169.
[6] L.M. Toth, G.D. Delcul, S. Dai, D.H. Metcalf, AIP conference proceedings 346 (1995) 617–625.
[7] L.M. Toth, G.D. Delcul, S. Dai, D.H. Metcalf, Space Nuclear Power Conference proceeding (1995) .
[8] S. Delpech, E. Merle-Lucotte, T. Auger, X. Doligez, D. Heuer, G. picard, Communication in GIF Symposium, Paris, France, 2009.
[9] J.W. Koger, ORNL 4832 (1972) .
[10] S. Delpech, C. Cabet, C. Slim, G. Picard, Mater. Today 13 (2010) 34–41.
[11] X. Doligez, PhD thesis, Infuence du retraitement physico-chimique du sel combustible sur le comportement du MSFR et sur le dimensionnement de son unité de retraitement, Université de Grenoble, France, 2010.
[12] S. Delpech, E. Merle-Lucotte, D. Heuer, M. Allibert, V. Ghetta, C. Le-Brun, X. Doligez, G. Picard, J. Fluo. Chem 130 (2009) 11–17.
[13] L. Massot, P. Chamelot, L. Cassayre, P. Taxil, Electrochim. Acta 54 (2009) 6361–6366.
[14] C. Nourry, L. Massot, P. Chamelot, P. Taxil, Electrochim. Acta 53 (2008) 2650–2655.
[15] O. Lemoine, PhD thesis, Electro-synthèse de UF_6 en milieu de sels fondus, Université de Toulouse, France, 2011.